

## CFD-SUPPORTED DATA REDUCTION OF HOT-WIRE ANEMOMETRY SIGNALS FOR COMPRESSIBLE ORGANIC VAPOR FLOWS

**Leander Hake**

Muenster University of Applied Sciences  
48565 Steinfurt, Germany

**Stephan Sundermeier**

Muenster University of Applied Sciences  
48565 Steinfurt, Germany

**Stefan aus der Wiesche**

Muenster University of Applied Sciences  
48565 Steinfurt, Germany

**Aurélien Bienner**

Art et Metiers Institute of Technology  
151 Bd. de l'Hopital, Paris, France

**Xavier Gloerfelt**

Art et Metiers Institute of Technology  
151 Bd. de l'Hopital, Paris, France

**Camille Matar**

Sorbonne University  
4 place Jussieu, Paris, France

**Paola Cinnella**

Sorbonne University  
4 place Jussieu, Paris, France

### ABSTRACT

For obtaining turbulent fluctuations in compressible organic vapor flows, computational fluid dynamics (CFD) analysis tools were used to support the data reduction process of hot-wire anemometry signals. It was found that CFD can help during the calibration process of actual hot-wire probes operated in the constant-temperature mode. Such an approach is beneficial for determining the dependency of the sensitivity coefficients on Reynolds and Mach numbers. Due to the small Kolmogorov scales, corrections are needed for probes with finite wire lengths. The experimental and numerical analysis considering the decay of turbulence downstream a grid indicated that the correction scheme proposed by Wyngaard leads to consistent results for compressible organic vapors. The new developments provide recommendations for obtaining turbulent quantities of compressible organic vapor flows utilizing hot-wire anemometry.

### NOMENCLATURE

*A* heat transfer correlation constant  
*B* heat transfer correlation constant  
*C* correction factor, -  
*d* turbulence grid rod diameter, m  
*d* wire diameter, m  
*E* electrical voltage, V  
*E* turbulent spectrum, -  
*k* wave number, 1/m  
*Kn* Knudsen number, -

*l* wire length, m  
*M* turbulence grid mesh size, m  
*M* Mach number, -  
*m* mass flow rate, kg/s  
*n* Reynolds number exponent, -  
*n* normal coordinate (dimensionless), -  
*Nu* Nusselt number, -  
*Pr* Prandtl number, -  
*Re* wire Reynolds number ( $Re = d \rho U/\mu$ ), -  
*S* sensitivity coefficient, -  
*T* temperature, K  
*t* time, s  
*U* (mean) velocity, m/s  
*x* distance or coordinate, m  
*y* coordinate, m

### Greek Symbols

$\gamma$  isentropic exponent, -  
 $\Lambda$  integral length scale, m  
 $\eta$  Kolmogorov length scale, m  
 $\mu$  dynamic viscosity, Pa s  
 $\rho$  density, kg/m<sup>3</sup>  
 $\tau$  overheat ratio, -

### Subscripts/Superscript

*o* total  
*w* wire  
+ normalized, dimensionless

### Mathematical Symbols

$\bar{X}$  mean (average) part of variable *X*  
 $X'$  fluctuating part of variable *X* ( $X = \bar{X} + X'$ )

## INTRODUCTION

The hot-wire anemometry (HWA) is an essential tool for measuring turbulent fluctuations. However, a correct data reduction is inherently challenging, especially in compressible flows. The fundamental problem is that velocity, density, and temperature fluctuations affect a single scalar electrical output signal of a probe placed in a flow. Without further model assumptions of the flow and its turbulent behavior, it is impossible to resolve that issue. Furthermore, the finite length of wires introduces the need for corrections to cover the corresponding attenuation effect, as discussed by Smolyakov and Tkachenko [1].

Flows of organic vapors consisting of complex molecules are typically characterized by compressibility and non-perfect gas dynamics. Due to their high density and velocity levels, relatively small Kolmogorov length scales are achieved in organic vapor flows. These issues increase the difficulties of applying the hot-wire anemometry in such flows and make calibration processes vastly costly and time-consuming. Such flow is present in turbomachinery for organic Rankine cycle (ORC) power systems.

Since the advent of direct numerical simulations (DNS), large-eddy simulations (LES), and sophisticated turbulence modeling, it is now possible to study turbulent fluctuations and their impact on wires numerically in detail. Following this path, using reliable computational fluid dynamics (CFD) methods during the calibration and the data reduction process offers a chance to attack the fundamental metrological problem posed in HWA and to reduce the calibration efforts by a combination of experimental and numerical data.

## HOT-WIRE HEAT TRANSFER

Fundamentals of heat transfer from hot-wires and hot-wire anemometry in compressible flows can be found in [2-5]. This section lists only the central relations and correlations used in the present work.

The convective heat transfer from a long, heated cylinder of length  $l$  and diameter  $d$  can be expressed by a Nusselt number

$$Nu = Nu(Re, M, Pr, Kn, \tau, \frac{d}{l}) \quad (1)$$

which is generally a function of the wire Reynolds number  $Re$ , Mach number  $M$ , Prandtl number  $Pr$ , Knudsen number  $Kn$ , overheat ratio  $\tau$ , and aspect ratio  $d/l$ . For a given cylinder and a given fluid, the Nusselt number  $Nu = Nu(Re, M, \tau)$  depends only upon the Reynolds number, Mach number, and the overheat ratio because the Knudsen number can be substituted by

$$Kn = \frac{M}{Re} \sqrt{\frac{\gamma\pi}{2}} \quad (2)$$

In the case of an organic vapor with a large density, the Reynolds number  $Re$  is typically high. Hence, the Knudsen number tends to have a very low value indicating that the organic vapor can be treated as a continuum.

Traditionally, a semi-empirical correlation

$$Nu = A(M, \tau) + B(M, \tau)Re^n \quad (3)$$

with empirical functions  $A$  and  $B$  and exponent  $n$  has proven its reliability. By relating the heat transfer rate to the electrical voltage output  $E$  of the constant-temperature anemometer (CTA), it can be shown that the Nusselt number  $Nu$  is proportional to  $E^2$ . Following de Souza and Tavoularis [6], it is hence appropriate to use the semi-empirical correlation

$$E^2 = A(M, T_o) + B(M, T_o)(\rho U)^n \quad (4)$$

for a fixed overheat ratio  $\tau$  and a known total fluid temperature  $T_o$ . The exponent  $n$  can often be well approximated by its "laminar" value  $n = 1/2$ .

A linearization of the heat transfer equation and the use of logarithmic derivatives yield the sensitivity coefficients

$$S_u = \left( \frac{\partial \ln E}{\partial \ln U} \right)_{\rho, T_o} \quad (5a)$$

$$S_\rho = \left( \frac{\partial \ln E}{\partial \ln \rho} \right)_{U, T_o} \quad (5b)$$

$$S_T = \left( \frac{\partial \ln E}{\partial \ln T_o} \right)_{\rho, U} \quad (5c)$$

for relating the voltage signal fluctuation  $E'$  to the velocity, density, and total temperature fluctuations:

$$\frac{E'}{E} = S_u \frac{U'}{U} + S_\rho \frac{\rho'}{\rho} + S_T \frac{T'_o}{T'_o} \quad (6)$$

For supersonic flow ( $M > 1.2$ ), Morkovin [4] has shown that the Mach number influence for the sensitivity coefficients is small and may be ignored. Then, the sensitivity coefficients for density and velocity become equal, and formally a simplified relation holds

$$\frac{E'}{E} = S_{\rho u} \frac{(\rho U)'}{(\rho U)} + S_T \frac{T'_o}{T'_o} \quad (7)$$

The equality  $S_u = S_\rho = S_{\rho u}$  was also observed by some authors [7, 8] in high subsonic for wires operated at a sufficiently high overheat ratio. Still, other studies [6, 9] indicated non-equal sensitivity coefficients. The equality of the two sensitivities coefficients significantly reduces the data reduction and calibration efforts, but it has to be proven individually for each hot-wire anemometer and flow situation. The identity  $S_u = S_\rho = S_{\rho u}$  requires, as a necessary condition  $(\partial \ln Nu / \partial \ln M)_{Re} = 0$  [5, 8]. This condition is always formally fulfilled in the limit case  $M = 0$  (i.e., incompressible flow). If the heat transfer coefficients  $A$  and  $B$  of Eq. (3) are functions of the Mach number  $M$ ,  $(\partial \ln Nu / \partial \ln M)_{Re} = 0$  is non-trivial (but formally possible).

## METHOD AND TEST CONFIGURATION

In the present experimental and numerical study, hot-wire probes operated in the constant-temperature mode were considered in a compressible flow of the organic vapor Novec 649 by 3M. Some thermodynamic data of Novec 649, a representative fluid for ORC applications, are listed in Table 1.

The experiments were done in the closed-loop organic vapor wind tunnel CLOWT test section (see Figure 1. CLOWT stands for closed-loop organic vapor wind tunnel. It permits the investigation of organic vapor flows at elevated temperature and pressure levels as representative of ORC power system applications. More details on the test facility CLOWT and its working principle can be found in previous publications [10-13]. Figure 1.a shows the entire test rig with the centrifugal compressor (blue colored), the basic test section with 2.5 m total length containing a second nozzle, the calibration test section (with cross area 50 mm x 100 mm), and a diffuser, Figure 1.b

**Table 1:** Thermodynamic data of Novec 649

Molecular formula	$\text{CF}_3\text{CF}_2\text{C}(\text{O})\text{CF}(\text{CF}_3)_2$
Molecular weight	316 g/mol
Boiling point (at 0.1 MPa)	322 K (49 °C)
Critical temperature	442 K (169 °C)
Critical pressure	1.88 MPa
Heat of vaporization (at boiling point)	88 kJ/kg
Thermal decomposition	573 K (300 °C)

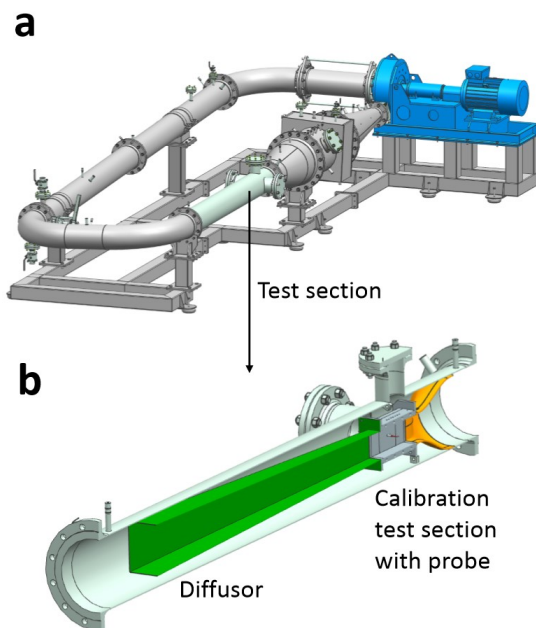


**Figure 1:** Test facility CLOWT (a) and details of the basic test tube (b)

This test facility was used for the calibration of hot-wire probes. Details about the experimental calibration can be found in a recent publication [14]. With certain restrictions, the wind tunnel operational envelope enabled the independent variation of Mach and Reynolds numbers and total temperature. The envelope of the wind tunnel in the  $Re, M$ -plane is shown in Figure 2. For a wire diameter of  $d = 10 \mu\text{m}$ , wire Reynolds numbers of well above  $Re = 1000$  could be achieved due to the high density of Novec 649.

Two different hot-wire probe designs (gold-plated tungsten wires) were used for the investigations, as shown in Figure 3. Whereas the larger wire probes (wire diameter  $10 \mu\text{m}$ , wire length 4 mm) were already successfully applied in recent studies [10, 14], smaller probes with wire diameter  $5 \mu\text{m}$  and wire length of 1 mm were employed in the present campaign, too. Using two different wire sizes with the same electrical resistance enabled an independent test of the applied correction scheme for the finite wire effects. A commercial and a self-designed electronic circuit were used for the anemometers. Different filter settings and sampling rates were considered for obtaining the data. The data reduction and evaluation were performed using MATLAB routines.

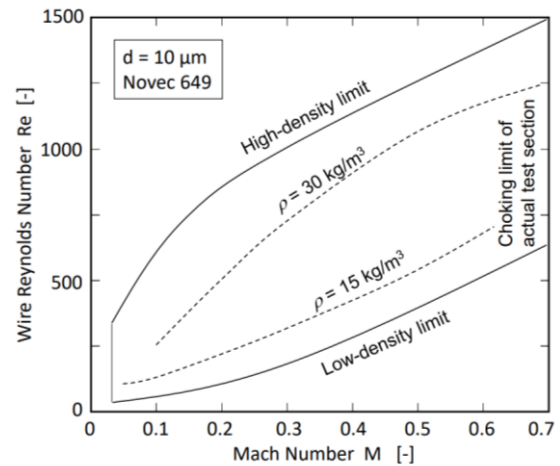


**Figure 2:** Operation envelope of CLOWT for calibration of hot-wire probes with  $d = 10 \mu\text{m}$

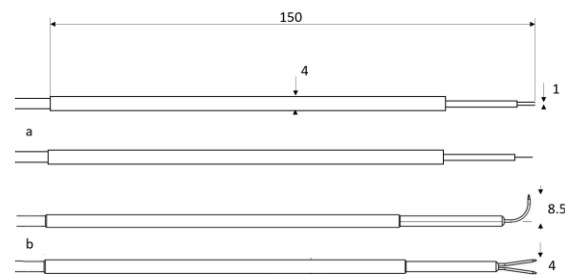


**Figure 3:** Hot-wire probes (dimensions in mm): a  $5 \mu\text{m}$ -1mm (Dantec) b  $10 \mu\text{m}$ -4mm (SVMtec)

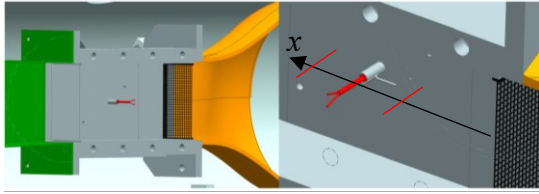


**Figure 4:** Turbulence grid configuration (left) and red-marked probe stations (right)

As a practical test for HWA, the decay of turbulence downstream of a grid was selected. Following Davidson [15], predicting the evolution of freely decaying, homogeneous turbulence is probably the most difficult problem in turbulence because, in that case, only the "naked non-linearity" of the involved dynamics is present. Grid turbulence is the archetypal example of that theoretical ideal. In the present context, it offered an excellent benchmark case for assessing the performance of the HWA. Figure 4 shows details of the turbulence grid test section. At the entrance of the test section, a grid with a rod diameter of  $d = 1$  mm and mesh size  $M = 4$  mm) was placed. At three different stations downstream of the grid, hot wire probes were placed. Using Taylor's hypothesis, the decrease of turbulent fluctuations with increasing distance  $x$  could be related to the decay of isotropic turbulence in time.

#### COMPUTATIONAL METHOD

Since relatively high Reynolds numbers were encountered in organic vapor flows, the influence of the turbulent wake on heat transfer properties of the hot wire was analyzed by means of Large-Eddy Simulations (LES). A spanwise slice of the cylinder was considered, and an in-house finite-difference code was used to solve the compressible Navier-Stokes equations written in curvilinear coordinates. The inviscid fluxes were discretized by means of 10th-order standard centered differences, whereas 4th-order was used for viscous fluxes. The scheme was supplemented with a 10th-order selective filtering to eliminate grid-to-grid unresolved oscillations. A four-stage Runge-Kutta algorithm was used for time integration. A high-order Implicit Residual Smoothing method [15] was implemented to enlarge the stability and allow the use of larger timesteps. No-slip conditions were applied on the solid surface, and non-reflecting Tam and Dong's conditions were imposed at the free boundaries. Periodicity was enforced in the spanwise direction. The Peng-Robinson-Stryjek-Vera equation of state and the Chung-Lee-Starling transport property model were applied [16].

The compressible filtered Navier-Stokes equations were discretized on a structured multi-

block curvilinear mesh fitted around a circular cylinder representing the hot-wire. The mesh was extruded in the spanwise direction at a distance  $\pi d$ , where  $d$  is the wire diameter. The computational domain extends over  $30d$  in the streamwise and  $20d$  in the normal directions, where the cylinder center was located at  $10d$  from the inlet. The mesh consisted of 12 blocks and corresponded to an "H-O-H" configuration. The total number of points contained in a  $x - y$  plane was  $68.6 \times 10^3$ , and 48 planes were used in the spanwise direction. This led to a total number of  $3.3 \times 10^6$  grid points. The wire surface was discretized with 210 points, with a first cell height of  $y/d = 2 \times 10^{-3}$ . This resolution was based on preliminary validations carried out for the well-known benchmark test [17] at  $Re = 3900$ , where the flow transitions in the very near wake. A close-up view of the mesh near the cylinder and an illustration of the wake flow are shown in Figure 5 and Figure 6, respectively.

The surface temperature of the hot-wire was kept constant (isothermal conditions) with a constant overheat ratio of  $\tau = 1.63$ , corresponding to the experimental setup. The local Nusselt number was computed through

$$Nu = \frac{\partial T^+}{\partial n} \quad \text{with } T^+ = \frac{T - T_w}{T_{in} - T_w} \quad (8)$$

For comparing time-averaged quantities with corresponding experimental data, the numerical data were integrated over at least 35 vortex shedding events, corresponding to a non-dimensional time  $t^+ = d/U_{in} \geq 350$  for all cases. A spanwise average was also performed to converge the statistics further.

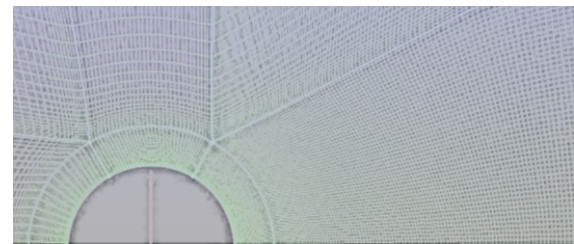


**Figure 5:** Illustration of the computational mesh

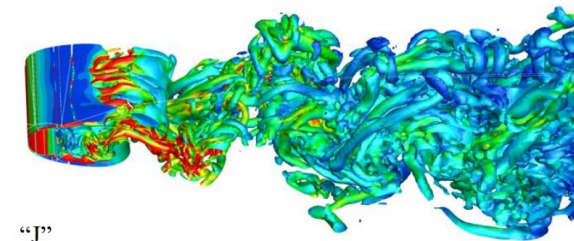


**Figure 6:** Instantaneous contours using the Q-criterion (colored by the vorticity magnitude) for illustrating the flow downstream of the hot-wire (case "J": diameter  $d = 10 \mu\text{m}$ ,  $Re = 1240$ ,  $M = 0.69$ )

The compressible homogeneous isotropic turbulence decay simulations were performed on a cubic computational domain of dimensions  $[0; 6\pi\Lambda]^3$  which  $\Lambda$  represents the integral length scale. For initialization of the decay simulations, the von Kàrmàn-Saffman spectrum was assumed:

$$E(k) = \alpha \frac{u^2}{k_e} \frac{\left(\frac{k}{k_4}\right)^4}{\left(1 + \left(\frac{k}{k_4}\right)^2\right)^{17/6}} \exp\left(-a\left(\frac{k}{k_\eta}\right)^b\right) \quad (9)$$

## RESULTS: HOT-WIRE CALIBRATION

In the first part of the present study, an experimental calibration study's outcome was compared with the CFD's predictions. The background turbulence level in the test section was of order 0.1 up to 0.2 % for the calibration. The total temperature level was maintained constant at fixed total temperature levels within 0.1 K.

For the large probe (10  $\mu\text{m}$  wire diameter and 4 mm length), it was found that the sensitivity coefficients for density and velocity were essentially identical. Such an observation must formally correspond to a negligible Mach number dependency of the Nusselt number for a fixed Reynolds number. This behavior was already observed, see Figure 7.

Figure 8 shows some averaged Nusselt number distributions against the circumferential angle of the wire. An inspection of Figure 8 indicates that the Mach number dependency was absent in the case for a fixed wire Reynolds number of  $Re = 1240$ : the local Nusselt number distributions collapsed to a single profile. However, a significant Reynolds number dependency can already be observed in the numerical results plotted in Figure 8 because the Nusselt number distributions for nearly the same Mach number ( $M = 0.67$  and  $M = 0.69$ ) but different Reynolds numbers ( $Re = 717$  and  $Re = 1240$ ) did not collapse. A comparison between measured and numerically predicted Nusselt numbers is shown in Figure 9.

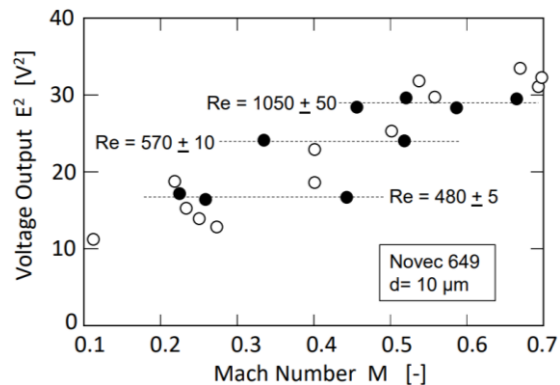


**Figure 7:** Voltage output against Mach number (solid symbols and dotted lines highlight fixed Reynolds number levels)

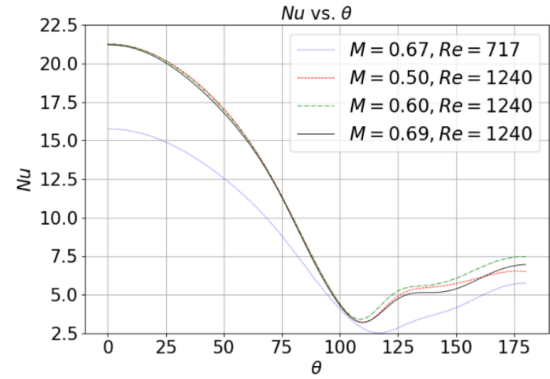


**Figure 8:** Averaged computed Nusselt number distributions for some Reynolds and Mach numbers

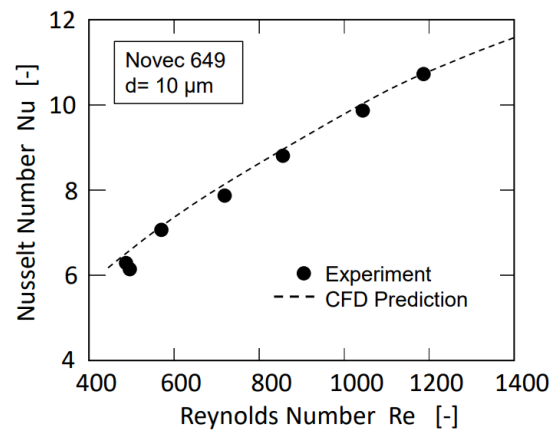


**Figure 9:** Measured and predicted averaged Nusselt number for a hot wire placed in high subsonic stream of an organic vapor

The agreement shown in Figure 9 is so good that CFD can substantially support the calibration process: the huge field of operational parameters (Reynolds number, Mach number, total temperature, wire temperature, density level) to be considered in a calibration study for the compressible flow of an organic vapor can be covered numerically. Then, some experimental data are only required for validating the CFD method. This hybrid approach worked for sufficiently long wires at high overheat levels. For short wires, the three-dimensional flow field caused by the probe and its prongs would lead to prohibitive high computational running times and efforts.

If the sensitivity coefficients regarding density and velocity are identical, the relation

$$\frac{\overline{E'^2}}{\overline{E}^2} = S_T^2 \frac{\overline{(T_t)'^2}}{\overline{(T_t)}^2} + S_{\rho u}^2 \frac{\overline{(\rho u)'^2}}{\overline{(\rho u)}^2} + 2S_{\rho u} S_T \frac{\overline{(\rho u)' T_t'}}{\overline{(\rho u)} \overline{T_t}} \quad (10)$$

holds for the rms-values of the turbulent quantities. In the case of an organic vapor with  $\gamma = 1$ , the total temperature contribution vanishes due to a general relation [5] for fluctuation modes in a gas:

$$\frac{\overline{T}^{1/2}}{\overline{T}^2} = (\gamma - 1)^2 M^4 \frac{\overline{u}^{1/2}}{\overline{u}^2} \quad (11)$$

Then, only the mass flux contribution and the last term in relation (10) contribute to the electrical voltage fluctuations. In any case, the complete calibration of a probe requires specific knowledge about the fluctuation modes (i.e., the rms-contributions of the different thermodynamic variables). Direct numerical simulations resolving the turbulent fluctuations offer a great potential to circumvent this severe metrological problem. It is then possible to conduct a model-based calibration by assuming numerically found relations for the rms-contributions in Eq. (10).

### RESULTS: CORRECTION SCHEME

In the second part of the present study, the reliability of the correction scheme was assessed for hot-wires when applied to obtaining turbulent fluctuations. The high density of the organic vapor led to relatively high wire and grid Reynolds numbers. Due to the resulting small Kolmogorov scale  $\eta$ , corrections were needed to account for the systematic attenuation of high-frequency signals by probes with finite wire lengths. That issue is absent in the case of a static calibration using a wind tunnel with low background turbulence, as conducted in the first part of this study.

It was assumed that the correction scheme proposed by Wyngaard [18], initially developed for isotropic turbulence in incompressible flows, would be applicable for the high-subsonic flow of organic vapor, too. Following Wyngaard [1, 18], the correction factor  $C$  for the streamwise rms-values was calculated for the limit case  $\eta/l = 0$  assuming the spectrum (9). Due to the small Kolmogorov length scale  $\eta$  in an organic vapor at high speeds, any practical wire is much longer. This led to the semi-empirical correlation

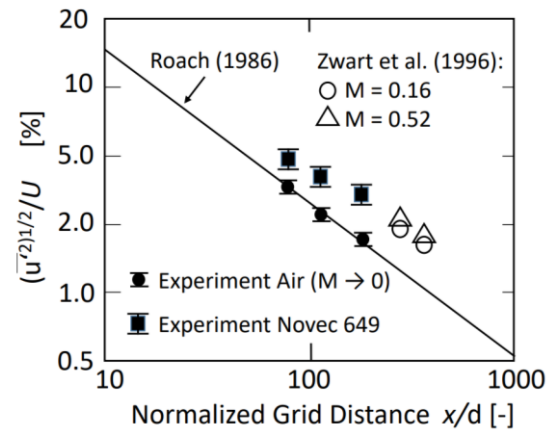
$$C = \frac{\overline{\rho u'^2}}{\overline{\rho u'^2}_{measured}} = 1.00 + 0.33 \frac{l}{\Lambda} \quad (12)$$

Relation (12) states that the "true" rms-values are systematically higher than the measured ones. For hot-wires with  $l \ll \Lambda$ , there is no need to correct the data.

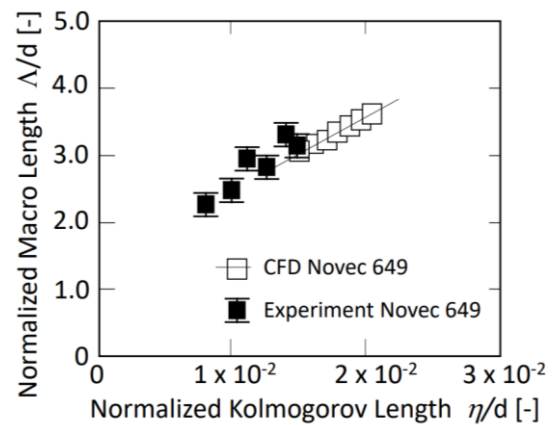
A natural test case of assessing wire length correction schemes is the decay of turbulence downstream of a grid with mesh size  $M$  and grid rod diameter  $d$ . The present measurements were performed using two different wires, see Figure 3, and a turbulence grid with a mesh size of  $M = 4$  mm and  $d = 1$  mm. Since the integral length scale  $\Lambda$  is typical of the same order as the mesh size  $M$  [19], the long wire ( $l = 4$  mm) was characterized by a substantial attenuation effect. Even the smaller wire with  $l = 1$  mm was long in terms of turbulent motions, and an attenuation effect was expected, too.

Figure 10 shows the measured turbulence intensities (streamwise direction) against the normalized distance  $x/d$ . Whereas the data for air (at a very low Mach number  $M < 0.10$ ) were in excellent agreement with a correlation suggested by Roach [19], the data obtained for Novec 649 at higher subsonic flow ( $0.16 < M < 0.5$ ) were systematically higher than predicted by the incompressible correlation. However, the new Novec 649 data showed the same trend as the data obtained for air in a similar compressible flow experiment performed by Zwart et al. [20].

To check the assumptions made for deriving the correction correlation (12), the experimentally obtained behavior of the turbulent length scales  $\Lambda$  and  $\eta$  were compared with the outcome of a direct numerical simulation using the same thermodynamic initial state as done in the grid experiments, see Figure 11. Although the numerical simulation covered a decay with larger length scales, the same behavior as observed in the experiments was found.



**Figure 10:** Turbulence decay downstream of a grid in compressible flow and comparison with incompressible flow



**Figure 11:** Experimentally and numerically obtained behavior of the length scales for grid-generated turbulence

Finally, the measured data were analyzed regarding their consistency. For instance, the measured turbulent intensities were  $Tu = 3.03\%$  and  $3.34\%$  for the probes with  $l = 4\text{ mm}$  and  $l = 1\text{ mm}$  for an integral length of about  $\Lambda \approx 3\text{ mm}$ . Using correlation (12), the ratio between the two values for  $Tu$  would be expected to be 0.88. In contrast, experimentally, a ratio of  $3.03/3.34 = 0.91$  was found. The remaining deviation was well within the general uncertainty level.

## SUMMARY AND OUTLOOK

Computational fluid dynamics (CFD) analysis tools were used to support the calibration and data reduction process of hot-wire anemometry signals to obtain turbulent fluctuations in compressible organic vapor flows.

It was experimentally found that due to the high overheat and Reynolds number levels, the sensitivity coefficients for density and velocity become essentially identical for a single hot-wire probe.

The experimental and numerical analysis considering the decay of turbulence downstream a grid indicated that the correction scheme proposed by Wyngaard leads to consistent results for compressible organic vapors.

The subject of an ongoing study is the application of hot-wire anemometry to flow through ORC turbine cascades.

## ACKNOWLEDGMENTS

This work was part of the Franco-German research project "REGAL-ORC" funded by ANR and DFG.

## REFERENCES

- [1] Smolyakov, A. V., Tkachenko, V. M., 1983, *The Measurement of Turbulent Fluctuations*, Springer Berlin
- [2] Kovasznay, L. S. G., 1950, *The Hot-Wire Anemometer in Supersonic Flows*, *J. Aeronautical Sciences*, vol. 17, pp. 565-584
- [3] Spangenberg, W. G., 1955, *Heat Loss Characteristics of Hot-Wire Anemometers at Various Densities in Transonic and Supersonic Flow*, NACA Tech. Note No. 3381
- [4] Morkovin, M. W., 1956, *Fluctuations and Hot-Wire Anemometry in Compressible Flows*, AGARDograph No. 24
- [5] Motallebi, F., 1994, *A Review of the Hot-Wire Technique in 2-D Compressible Flows*, *Prog. Aerospace Sci.*, vol. 30, 267-294
- [6] de Souza, F., Tavoularis, S., 1999, *Hot-Wire Response in High-Subsonic Flow*, *Proceedings AIAA 37<sup>th</sup> Aerospace Sciences Meeting and Exhibit*, Reno, Nevada, AIAA-99-0310
- [7] Horstman, C. C., Rose, W. C., 1977, *Hot-Wire Anemometry in Transonic Flow*, *AIAA Journal*, vol. 15, pp. 395-401
- [8] Rose, W. C., McDaid, E. P., 1977, *Turbulence Measurement in Transonic Flow*, *AIAA Journal*, vol. 15, pp. 1368-1370
- [9] Stainback, P. C., 1986, *Some Influences of Approximate Values for Velocity, Density and Total Temperature Sensitivities on Hot Wire Anemometer Results*, *Proceedings AIAA 24<sup>th</sup> Aerospace Sciences Meeting*, Reno, Nevada, AIAA-86-0506
- [10] Reinker, F., aus der Wiesche, S., 2021, *Application of Hot-Wire Anemometry in the High Subsonic Organic Vapor Flow Regime*, In: M. Pini et al. (Eds.): *NICFD 2020, ERCOFTAC Series 28*, pp. 135-143
- [11] Reinker, F., Kenig, E. Y., aus der Wiesche, S., 2018, *CLOWT: a multifunctional test facility for the investigation of organic vapor flows*, *Proc. ASME 2018 FEDSM*, Montreal, Canada (paper FEDSM2010-83076).
- [12] Reinker, F., Hasselmann, K., aus der Wiesche, S., Kenig, E. Y., 2016, *Thermodynamics and Fluid Mechanics of a Closed Blade Cascade Wind Tunnel for Organic Vapors*, *ASME J. Eng. Gas Turb. Power*, vol. 138, paper-ID 052601
- [13] Reinker, F., Kenig, E. Y., aus der Wiesche, S., 2019, *Closed Loop Organic Vapor Wind Tunnel CLOWT: Commissioning and Operational Experience*, *Proc. 5th ORC Conference*, Athens, Greece, paper-ID 47
- [14] Hake, L., Sundermeier, S., Cakievski, L., Bäumer, J., aus der Wiesche, S., Matar, C., Cinnella, P., Gloerfelt, X., 2022, *Hot-Wire Anemometry in High Subsonic Organic Vapor Flows*, *Proc. ASME Turbo Expo 2022*, Rotterdam, The Netherlands, paper GT2022-81689
- [15] Cinnella, P., Content, C., 2016, *High-Order Implicit Residual Smoothing time scheme for direct and large eddy simulations of compressible flows*, *J. Comp. Physics*, vol. 326, 1-29
- [16] Chung, T.H., Ajlan, M., Lee, L.L., Starling, K.E., 1988, *Generalized multiparameter correlation for nonpolar and polar fluid transport properties*, *Industrial Eng. Chemistry Res.*, vol. 27, 671-679.
- [17] Parnaudeau, P., Carlier, J., Heitz, D., Lamballais, E., 2008, *Experimental and numerical studies of the flow over a circular cylinder at Reynolds number 3900*, *Phys. Fluids*, vol. 20, 08510
- [18] Wyngaard, J. C., 1968, *Measurement of small-scale turbulence structure with hot wires*, *J. Scientific Instruments*, vol. 1, pp. 1105-1108
- [19] Roach, P. E., 1986, *The generation of nearly isotropic turbulence by means of grids*, *Heat Fluid Flow*, 8(2), 82-92.
- [20] Zwart, P. J., Budwig, R., Tavoularis, S., 1997, *Grid turbulence in compressible flow*, *Exp. Fluids*, 23, pp. 520-522.